A&A 407, L47–L50 (2003)
DOI: 10.1051/0004-6361:20030786

Astronomy & Astrophysics

The spinning-top Be star Achernar from VLTI-VINCI

A. Domiciano de Souza[1], P. Kervella[2], S. Jankov[3], L. Abe[1], F. Vakili[1,3], E. di Folco[4], and F. Paresce[4]

[1] Laboratoire Univ. d'Astroph. de Nice (LUAN), CNRS UMR 6525, Parc Valrose, 06108 Nice Cedex 02, France
[2] European Southern Observatory (ESO), Alonso de Cordova 3107, Casilla 19001, Vitacura, Santiago 19, Chile
[3] Observatoire de la Côte d'Azur, Département FRESNEL, CNRS UMR 6528, Boulevard de l'Observatoire, BP 4229, 06304 Nice, France
[4] European Southern Observatory (ESO), Karl-Schwarzschild str. 2, 85748 Garching, Germany

Received 5 May 2003 / Accepted 22 May 2003

Abstract. We report here the first observations of a rapidly rotating Be star, α Eridani, using Earth-rotation synthesis on the Very Large Telescope (VLT) Interferometer. Our measures correspond to a $2a/2b = 1.56 \pm 0.05$ apparent oblate star, $2a$ and $2b$ being the equivalent uniform disc angular diameters in the equatorial and polar direction. Considering the presence of a circumstellar envelope (CSE) we argue that our measurement corresponds to a truly distorted star since α Eridani exhibited negligible Hα emission during the interferometric observations. In this framework we conclude that the commonly adopted Roche approximation (uniform rotation and centrally condensed mass) should not apply to α Eridani. This result opens new perspectives to basic astrophysical problems, such as rotationally enhanced mass loss and internal angular momentum distribution. In addition to its intimate relation with magnetism and pulsation, rapid rotation thus provides a key to the Be phenomenon: one of the outstanding non-resolved problems in stellar physics.

Key words. techniques: high angular resolution – techniques: interferometric – stars: rotation – stars: emission-line, Be – stars: individual: Achernar

1. Introduction

The southern star Achernar (α Eridani, HD 10144, spectral type B3Vpe) is the brightest Be star in the sky. A Be star is defined as a non-supergiant B type star that has presented episodic Balmer lines in emission (Jaschek et al. 1981), whose origin is attributed to a CSE ejected by the star itself. Physical mechanisms like non-radial pulsations, magnetic activity, or binarity are invoked to explain the CSE formation of Be stars in conjunction with their fundamental property of rapid rotation. Theoretically, rotation has several consequences on the star structure (Cassinelli 1987). The most obvious is the geometrical deformation that results in a larger radius at the equator than at the poles. Another well established effect, known as gravity darkening or the von Zeipel effect for hot stars (von Zeipel 1924), is that both surface gravity and emitted flux decrease from the poles to the equator. Although well studied in the literature, the effects of rotation have rarely been tested against accurate enough observations (Reiners & Schmitt 2003; van Belle et al. 2001), a gap bridged by our interferometric observations of Achernar.

Send offprint requests to: A. Domiciano de Souza,
e-mail: Armando.Domiciano@obs-azur.fr

2. Observations and data processing

Dedicated observations of Achernar have been carried out during the ESO period 70, from 11 September to 12 November 2002, with quasi-uniform time coverage, on the VLT Interferometer (VLTI, Glindemann et al. 2003) equipped with the VINCI beam combiner (Kervella et al. 2003a). This instrument recombines the light from two telescopes in the astronomical K band, which is centered at 2.2 μm and covers 0.4 μm. The observable measured by VINCI is the squared coherence factor μ^2 of the star light. It is derived from the raw interferograms after photometric calibration using a wavelet based method (Ségransan et al. 1999). The reduction procedure is detailed by Kervella et al. (2003b) and has successfully been applied to dwarf stars observations with the VLTI (Ségransan et al. 2003). The instrumental value of μ^2 is then calibrated through the observation of stable stars with known angular diameters. The calibrators chosen for Achernar are presented in Table 1. The final product of the processing is the squared visibility V^2 of the object for each baseline projected on the sky ($B_{\rm proj}$). V^2 is directly related to the Fourier transform of the brightness distribution of the object via the Zernike-Van Cittert theorem. For these observations, two interferometric baselines were used, 66 m (E0-G1; azimuth 147°, counted from North to East) and 140 m (B3-M0; 58°), equipped with 40 cm siderostats (Fig. 1 left). Their orientations are almost perpendicular to each other giving an excellent configuration for the

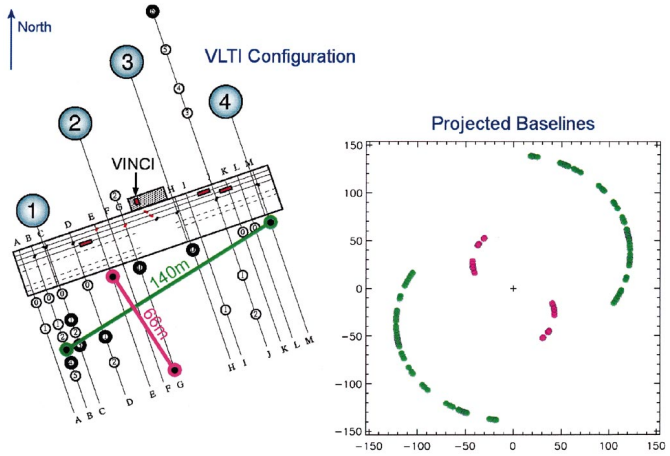

Fig. 1. VLTI ground baselines for Achernar observations and their corresponding projections onto the sky at different observing times. *Left*: Aerial view of VLTI ground baselines for the two pairs of 40 cm siderostats used for Achernar observations. Color magenta represents the 66 m (E0-G1; azimuth 147°, counted from North to East) and green the 140 m (B3-M0; 58°). *Right*: Corresponding baseline projections onto the sky ($B_{\rm proj}$) as seen from the star. Note the very efficient Earth-rotation synthesis resulting in a nearly complete coverage in azimuth angles.

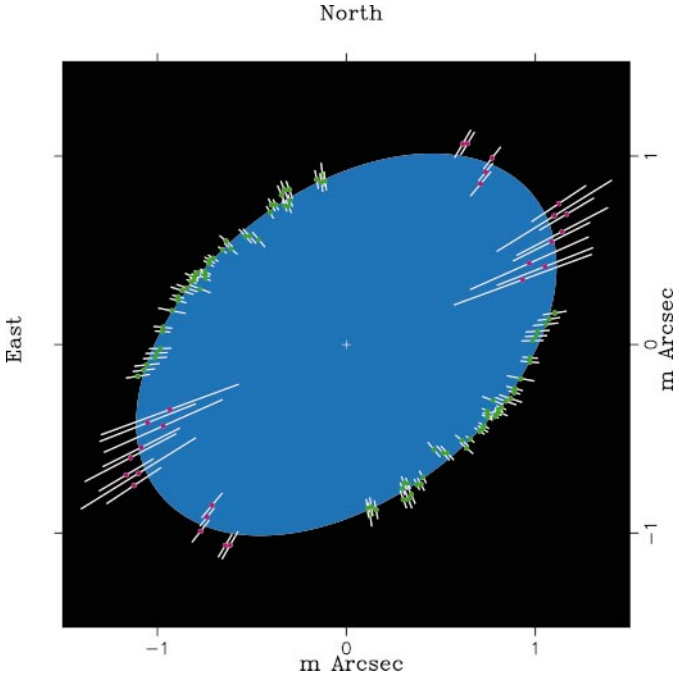

Fig. 2. Fit of an ellipse over the observed squared visibilities V^2 translated to equivalent uniform disc angular diameters. Each V^2 is plotted together with its symmetrical value in azimuth. Magenta points are for the 66 m baseline and green points are for the 140 m baseline. The fitted ellipse results in major axis $2a = 2.53 \pm 0.06$ milliarcsec, minor axis $2b = 1.62 \pm 0.01$ milliarcsec, and minor axis orientation $\alpha_0 = 39° \pm 1°$ (from North to East). The points distribution reveals an extremely oblate shape with a ratio $2a/2b = 1.56 \pm 0.05$.

detection of stellar asymmetries. Moreover, Earth-rotation has produced an efficient baseline synthesis effect (Fig. 1, right). A total of more than 20 000 interferograms were recorded on Achernar, and approximately as many on its calibrators, corresponding to more than 20 hours of integration. From these data, we obtained 60 individual V^2 estimates, at an effective wavelength of $\lambda_{\rm eff} = 2.175 \pm 0.003\,\mu$m.

3. Results

The determination of the shape of Achernar from our set of V^2 is not a straightforward task so that some prior assumptions need to be made in order to construct an initial solution for our observations. A convenient first approximation is to derive from each V^2 an equivalent uniform disc (UD) angular diameter $\oslash_{\rm UD}$ from the relation $V^2 = |2J_1(z)/z|^2$. Here, $z = \pi \oslash_{\rm UD}(\alpha) B_{\rm proj}(\alpha) \lambda_{\rm eff}^{-1}$, J_1 is the Bessel function of the first kind and of first order, and α is the azimuth angle of $B_{\rm proj}$ at different observing times due to Earth-rotation. The application of this simple procedure reveals the extremely oblate shape of Achernar from the distribution of $\oslash_{\rm UD}(\alpha)$ on an ellipse (Fig. 2). Since α, $B_{\rm proj}(\alpha)$, and $\lambda_{\rm eff}$ are known much better than 1%, the measured errors in V^2 are associated only to the uncertainties in $\oslash_{\rm UD}$. We performed a non-linear regression fit using the equation of an ellipse in polar coordinates. Although this equation can be linearized in Cartesian coordinates, such a procedure was preferred to preserve the original, and supposedly Gaussian, residuals distribution as well as to correctly determine the parameters and their expected errors. We find a major axis $2a = 2.53 \pm 0.06$ milliarcsec (mas), a minor axis $2b = 1.62 \pm 0.01$ mas, and a minor-axis orientation $\alpha_0 = 39° \pm 1°$. Note that the corresponding ratio $2a/2b = 1.56 \pm 0.05$ determines the equivalent star oblateness only in a first-order UD approximation. To interpret our data in terms of physical parameters of Achernar, a consistent scenario must be tailored from its basic known properties, so that we can safely establish the conditions where a coherent model can be built and discussed.

4. Discussion

Achernar's pronounced apparent asymmetry obtained in this first approximation, together with the fact that it is a Be star, raises the question of whether we observe the stellar photosphere with or without an additional contribution from a CSE.

For example, a flattened envelope in the equatorial plane would increase the apparent oblateness of the star if it were to introduce a significant infrared (IR) excess with respect to the photospheric continuum. Theoretical models (Poeckert & Marlborough 1978) predict a rather low CSE contribution in the K band especially for a star tilted at higher inclinations, which should be our case as discussed below. Indeed, Yudin (2001) reported a near IR excess (difference between observed and standard color indices in visible and L band centered at 3.6 μm) to be $E(V-L) = 0\overset{\rm m}{.}2$, with the same level of uncertainty. Moreover, this author reports a zero intrinsic polarization (p_*). These values are significantly smaller than mean values for Be stars earlier than B3 ($\overline{E(V-L)} > 0\overset{\rm m}{.}5$ and $\overline{p_*} > 0.6\%$), meaning that the Achernar's CSE is weaker than in other known Be stars. Further, an intermediate

Table 1. Relevant parameters of the calibrators of Achernar. $\oslash_{UD}$ is the equivalent uniform disc angular diameter. The value of $\oslash_{UD}$ for δ Phe and χ Phe is based on spectrophotometry (Cohen et al. 1999), while that for α PsA was measured separately with the VLTI and should appear in a forthcoming publication from one of us (E.F.).

Name	Spec. type	λ_{eff} (μm)	Baseline (m)	$\oslash_{UD}$ (mas)
δ Phe	K0IIIb	2.181	140	2.18 ± 0.02
α PsA	A3V	2.177	140	2.20 ± 0.07
χ Phe	K5III	2.182	66	2.69 ± 0.03

angular diameter of our elliptical fit (Fig. 2) is compatible with the $\oslash_{UD} = 1.85 \pm 0.07$ mas measured by Hanbury-Brown (1974) in the visible, in contrast to what is expected if the envelope were to contribute to our present IR observations. Finally, Chauville et al. (2001) report no emission in the Hγ line. Since the emission in Hγ and in the continuum are both formed roughly in the same layer of the CSE (Ballereau et al. 1995), the contribution from the nearby environment of the star should be considered below the limit of detection.

Of course, being classified as a Be star, Achernar can enhance the strength of its CSE due to episodic mass ejections, which are generally witnessed by increased Balmer line emission (e.g. de Freitas Pacheco 1982). This possibility was checked against a Hα spectrum (Leister & Janot-Pacheco 2003) taken in October 2002, during our VLTI-VINCI campaign presenting a photospheric absorption profile. To be sure that we observed a quiescent Achernar we synthesized a Hα profile from our model (Domiciano de Souza et al. 2002) compared to the observed line. We estimated the emission to be at most 3% across the whole line. Such an upper limit would correspond to a CSE emitting at most 12% of the photospheric continuum flux, due to free-free and free-bound emission (Poeckert & Marlborough 1978).

Thus, we assume hereafter that the observed asymmetry of Achernar mainly reflects its true photospheric distortion with a negligible CSE contribution. Under this assumption, and using the Hipparcos distance ($d = 44.1 \pm 1.1$ pc; Perryman et al. 1997), we derive an equatorial radius $R_{eq} = 12.0 \pm 0.4\ R_\odot$ and a maximum polar radius $R_{pol}^{max} = 7.7 \pm 0.2\ R_\odot$, respectively from $2a$ and $2b$ obtained from the elliptical fit on $\oslash_{UD}(\alpha)$. From simple geometrical considerations the actual polar radius R_{pol} will be smaller than R_{pol}^{max} for polar inclinations $i < 90°$, while R_{eq} is independent of i.

Based on these conclusions we applied our interferometry-oriented code (Domiciano de Souza et al. 2002) to Achernar. This code includes radiation transfer, the von Zeipel law ($T_{eff} \propto g_{eff}^{0.25}$, T_{eff} and g_{eff} being the effective temperature and gravity, respectively), and the Roche approximation (e.g. Roche 1837; Kopal 1987). In this approximation and noting that the stellar rotation must be kept smaller than its critical value, the adopted projected equatorial velocity $V_{eq} \sin i = 225$ km s^{-1} (Slettebak 1982) implies that $i > 46°$. At this limit T_{eff} and g_{eff} both attain zero at the equator, and the surface equipotential first derivatives become discontinuous. Therefore we chose to explore a parameter space between the representative limit

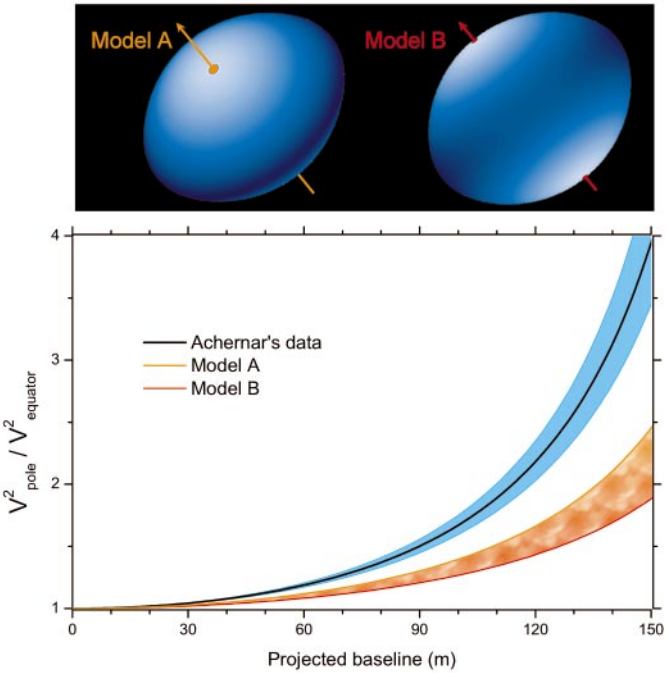

Fig. 3. Comparison of ratios of squared visibility curves between the polar and equatorial directions V_{pol}^2/V_{eq}^2. The black solid curve corresponds to V_{pol}^2/V_{eq}^2 for the elliptical fit on Achernar's data, together with the corresponding uncertainties. Simply speaking V_{pol}^2/V_{eq}^2 somehow reflects R_{eq}/R_{pol}^{max}, since interferometry is sensitive to the Fourier transform of the stellar brightness distribution. The colored region represents our attempt attain the black curve with our model for Achernar within the physically reasonable solutions A (orange; upper limit) and B (red; lower limit). This failure to reproduce the observations is a strong and direct indication that uniform rotation does not apply to rapidly rotating stars.

solution models A ($i = 50°$) and B ($i = 90°$). Table 2 summarizes the corresponding sets of fundamental parameters. Figure 3 clearly shows that the solutions enclosed between the models A and B cannot reproduce the observed highly oblate ellipse. We also checked, with negative result, whether the situation would improve significantly by varying the fundamental parameters of Achernar in a physically reasonable range (mass $\pm 1\ M_\odot$, $T_{pol} \pm 2000$ K, $V_{eq} \sin i \pm 25$ km s^{-1}).

Thus, in absence of Hα emission making a CSE contribution unlikely to reproduce the observed oblateness, the classical assumption of Roche approximation becomes questionable. Deviations from this gravitational potential and the presence of differential rotation, both intimately related to the internal angular momentum distribution, should be investigated. Indeed, several differential rotation theories predict surface deformations stronger than that of uniform rotation by considering that the angular velocity increases towards the stellar center. Two interesting examples are "shellular" rotation (Zahn 1992) and laws with angular momentum constant on cylinders (Bodenheimer 1971). In this context our result on Achernar's surface distortion should also impact other internal mechanisms like meridional circulation, turbulence, transport and diffusion of the chemical elements and angular momentum,

Table 2. Fundamental parameters for two limit solution models of Achernar. From the fixed parameters and in the Roche approximation, the minimum polar inclination is $i_{\rm min} = 46^\circ$ where $V_{\rm eq} = V_{\rm crit} = 311$ km s^{-1} and $R_{\rm eq} = 1.5\ R_{\rm pol}$. In addition to these parameters we adopted a linear limb darkening coefficient from Claret (2000) compatible with the variable effective temperature and gravity over the stellar surface. The equatorial effective temperature is much lower than the polar one due to the von Zeipel effect.

Fixed parameters	Adopted value	Comments
$T_{\rm pol}$	20 000 K	~B3V star
Mass	6.07 $M_\odot$	Harmanec (1988)
$V_{\rm eq} \sin i$	225 km s^{-1}	Slettebak (1982)
$R_{\rm eq}$	12.0 $R_\odot$	this work
Model dependent parameters	Values for Model A	Values for Model B
$T_{\rm eq}$	9500 K	14 800 K
i	50°	90°
$V_{\rm crit}$	304 km s^{-1}	285 km s^{-1}
$V_{\rm eq}$	$0.96 V_{\rm crit}$	$0.79 V_{\rm crit}$
$R_{\rm pol}$	8.3 $R_\odot$	9.5 $R_\odot$

increase of mass loss with rotation as well as anisotropies in the mass ejection and wind density from rotating stars (Maeder 1999; Maeder & Meynet 2000).

Finally, the highly distorted shape of Achernar poses the question of Be stars rotation rate. As argued by several authors (e.g. Cassinelli 1987; Owocki 2003) the formation of out-flowing discs from Be stars remains their central puzzle, where rapid rotation is the crucial piece. Struve's (1931) original vision of a critically rotating star, ejecting material from its equator, has been discarded in the past by observing that Be stars rotate at most 70% or 80% of their critical velocity (typically ~500 km s^{-1} for a B0V star). However, this statistically observed limit might be biased by the fact that close to or beyond such velocities the diagnosis of Doppler-broadened spectral lines fails to determine the rotation value due to gravity darkening (Owocki 2003; Townsend 1997). We believe that only direct measures of Be star photospheres by interferometry can overcome the challenge to prove whether these objects rotate close, to a few percent, of their critical velocity or not. This have a profound impact on dynamical models of Be stars CSE formation from rapid rotation combined to mechanisms like pulsation, radiation pressure of photospheric hot spots, or expelled plasma by magnetic flares.

Acknowledgements. A.D.S., P.K. and L.A. acknowledge CAPES-Brazil, ESO and CNES-France for financial support respectively. The authors acknowledge support from D. Mourard and his team from OCA-France. LUAN is supported by UNSA and CNRS. Observations with the VLTI became possible thanks to the VLTI team. We are grateful to Drs. N. V. Leister and E. Janot-Pacheco for Achernar's spectra.

References

Ballereau, D., Chauville, J., & Zorec, J. 1995, A&AS, 111, 423
Bodenheimer, P. 1971, A&A, 167, 153
Cassinelli, J. P. 1987, in Physics of Be stars, ed. A. Slettebak, & T. P. Snow (Cambridge: Cambridge Univ. Press), 106
Chauville, J., Zorec, J., Ballereau, D., et al. 2001, A&A, 378, 861
Claret, A. 2000, A&A, 363, 1081
Cohen, M., Walker, R. G., Carter, B., et al. 1999, AJ, 117, 1864
de Freitas Pacheco, J. A. 1982, MNRAS, 199, 591
Domiciano de Souza, A., Vakili, F., Jankov, S., Janot-Pacheco, E., & Abe, L. 2002, A&A, 393, 345
Glindemann, A., Algomedo, J., Amestica, R., et al. 2003, Proc. SPIE, 4838, 89
Hanbury Brown, R., Davis, J., & Allen, L. R. 1974, MNRAS, 167, 121
Harmanec, P. 1988, Bull. Astron. Inst. Czechoslovakia, 39, 329
Jaschek, M., Slettebak, A., & Jaschek, C. 1981, Be Star Newsletter, 4, 9
Kervella, P., Gitton, Ph., Ségransan, D., et al. 2003a, Proc. SPIE, 4838, 858
Kervella, P., Thévenin, F., Ségransan, D., et al. 2003b, A&A, 404, 1087
Kopal, Z. 1987, Ap&SS, 133, 157
Leister, N. V., & Janot-Pacheco, E. 2003, private commun.
Maeder, A. 1999, A&A, 347, 185
Maeder, A., & Meynet, G. 2000, A&ARv, 38, 143
Owocki, S. P. 2003, Proc. IAU Symp. 215, ed. A. Maeder, & P. Eenens, in press
Perryman, M. A. C., Lindegren, L., Kovalevsky, J., et al. 1997, A&A, 323, L49
Poeckert, R., & Marlborough, J. M. 1978, ApJS, 38, 229
Reiners, A., & Schmitt, J. H. M. M. 2003, A&A, 398, 647
Roche, E. A. 1837, Mém. de l'Acad. de Montpellier (Section des Sciences), 8, 235
Ségransan, D., Kervella, P., Forveille, T., & Queloz, D. 2003, A&A, 397, L5
Ségransan, D., Forveille, T., Millan-Gabet, C. P. R., & Traub, W. A. 1999, ASP Conf. Ser., 194, 290
Slettebak, A. 1982, ApJ, 50, 55
Struve, O. 1931, ApJ, 73, 94
Townsend, R. H. D. 1997, Ph.D. Thesis, Univ. College London
van Belle, G. T., Ciardi, D. R., Thompson, R. R., Akeson, R. L., & Lada, E. A. 2001, ApJ, 559, 1155
von Zeipel, H. 1924, MNRAS, 84, 665
Yudin, R. V. 2001, A&A, 368, 912
Zahn, J.-P. 1992, A&A, 265, 115